

Hall effects on local structures in decaying MHD turbulence

Hideaki MIURA and Dan. HORI¹⁾

Department of Simulation Science, National Institute for Fusion Science, Gifu 509-5292, Japan

¹⁾*Japan Aerospace Exploration Agency, Sagamihara, Kanagawa 229-8510, Japan*

(Received: 27 August 2008 / Accepted: 18 November 2008)

Influences of the Hall effects on local structures in magnetohydrodynamic turbulence are studied through the direct numerical simulations of decaying isotropic turbulence. Direct comparisons of the numerical results between the incompressible, single-fluid- and the Hall-magnetohydrodynamic equations reveal that the high-wavenumber region of the magnetic energy spectrum is considerably modified by the Hall effects. It is also shown that the structures which are composed of low-wavenumber velocity components are modified by the Hall effect from the sheet to tubular structures. It suggests that the basic plasma motions in MHD turbulence can be modified from shearing to swirling motions by the Hall effect.

Keywords: isotropic turbulence, small scale structures, Hall effects

1. Introduction

The single-fluid magnetohydrodynamic (MHD) equations have been applied to study many phenomena, including instabilities and/or turbulence, since many plasma phenomena are well described by the MHD equations. However, some of the phenomena can be out of the scope of the equations, and roles of two-fluid effects have attracted attention in some research areas such as fusion plasmas [1,2] and astrophysical plasmas [3,4].

One of the simplest fluid models of plasma motions with two-fluid effect is the incompressible Hall MHD equations, which can be described as

$$\frac{\partial \mathbf{u}}{\partial t} = -(\mathbf{u} \cdot \nabla) \mathbf{u} - \nabla p + \mathbf{j} \times \mathbf{B} + \nu \nabla^2 \mathbf{u}, \quad (1)$$

$$\frac{\partial \mathbf{B}}{\partial t} = \nabla \times [(\mathbf{u} - \epsilon \mathbf{j}) \times \mathbf{B}] + \eta \nabla^2 \mathbf{B}, \quad (2)$$

where \mathbf{B} is the magnetic field (normalized by a representative value B_0), $\mathbf{j} = \nabla \times \mathbf{B}$ is the current (normalized by B_0/L_0 ; L_0 is the characteristic length), \mathbf{u} is the velocity (normalized by the Alfvén speed $V_A = B_0 / \sqrt{\mu_0 n_i M_i}$; μ_0 is the permeability of vacuum, M_i is the ion mass and n_i is the ion number density, which is assumed to be constant for simplicity), ν is the viscosity and η is the resistivity (normalized by $V_A L_0$), and p is the pressure (normalized by B_0^2 / μ_0). The velocity field \mathbf{u} satisfies the incompressible continuity equation $\nabla \cdot \mathbf{u} = 0$ and the pressure p is given as a solution of the Poisson equation which comes from the divergence of eq.(1). The Hall parameter is given as $\epsilon = l_i / L_0$ where $l_i = \sqrt{M_i / \mu_0 n_i e^2}$ (e is an elementary charge) is the ion skin depth.

Properties of the Hall MHD equations and/or Hall MHD turbulence has been studied numerically as well as theoretically. [2,4-7] In our previous work [7], the authors have proposed a possible new scaling of the magnetic energy spectra in the Hall MHD turbulence, in which the magnetic energy spectrum is scaled by $k^{-7/3}$ in the high-wavenumber region. Although we have carried out direct

numerical simulations (DNSs) of the Hall MHD equations to study the turbulent spectra, the numerical resolution are limited and the scaling property remains as a conjecture.

The purposes of this article are twofolds. The first one is to obtain further insights on the scaling properties of the Hall MHD turbulence through the DNSs. The other one is to clarify effects of the Hall term on local structures. For these purposes we carry out DNSs of both the single-fluid MHD and Hall MHD decaying isotropic turbulence. Since the isotropic turbulence is an idealized system in the limit of small-scales, the DNSs are essentially dissipative. The equations are discretized by means of the pseudo-spectral method with 2/3-truncation de-aliasing technique under the triple-periodic boundary condition and marched into the time direction by the use of the Runge-Kutta-Gill scheme. The initial condition is given by the energy spectrum proportional to $k^2 \exp(-(k/k_0)^2)$ (here $k_0 = 2$) and random phases both for the velocity and magnetic fields. The number of grid points is $N^3 = 512^3$. The parameters are set as $\epsilon = 0.05$, $\nu = \mu = 2 \times 10^{-3}$, aiming to put the ion skin depth in between the energy injection scale k_0 and the dissipation scale.

2. Numerical Simulations

In Fig.1(a), the mean kinetic energy $E_K = \langle \mathbf{u}^2 \rangle / 2$ and the mean magnetic energy $E_M = \langle \mathbf{B}^2 \rangle / 2$ are plotted as a function of the time for the MHD and the Hall MHD simulations, respectively, where $\langle \cdot \rangle$ denotes the volume average. The thick lines represent the total energy $E_T = E_K + E_M$. While the the total energy E_T decays monotonically both in the MHD and the Hall MHD runs, the $E_K(E_M)$ increases (decreases) at the initial phase of the simulations, showing that there exists an energy exchange between E_K and E_M . The increase of E_K and decrease of E_M are clearer in the Hall MHD simulations than in the MHD simulations, suggesting the enhancement of the energy exchange by the Hall effect. The time evolutions of the enstrophy $Q = \langle \omega^2 \rangle$ where $\omega = \nabla \times \mathbf{v}$ is the vorticity and the current $J = \langle \mathbf{j}^2 \rangle$ are

author's e-mail: miura.hideaki@nifs.ac.jp

shown in Fig.1(b). The thick lines denote $Q + J$. Since we set $\nu = \eta$ in our DNS, the total dissipation rate $\epsilon_T = \nu Q + \eta J$ is proportional to $Q + J$. Here we compare the two kinds of simulations at the time when ϵ_T is the same to each other, that is $t = 1$ for the MHD simulation and $t = 1.04$ for the Hall MHD simulation.

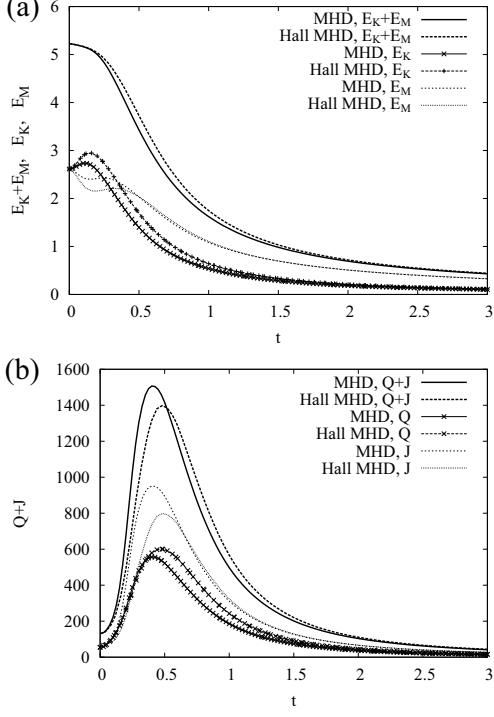


Fig. 1 (a)Time evolutions of the kinetic energy E_T , magnetic energy E_M and the total energy E_T . (b)Time evolutions of the enstrophy Q , current J and sum of them $Q + J$.

In Fig.2(a), the kinetic and magnetic energy spectra, $E_K(k)$ and $E_M(k)$ respectively, of the MHD simulation at $t = 1$ are shown. Here k is the wavenumber. Fig.2(b) is the Hall MHD counterparts at $t = 1.04$. Hereafter we omit the time stamps of the simulations, assuming $t = 1$ for the MHD simulation and 1.04 for the Hall MHD simulation. The spectra $E_K(k)$ and $E_M(k)$ are compensated by some typical powers of the wavenumber as $k^{5/3}E_K(k)$ (white boxes), $k^{5/3}E_M(k)$ (the black boxes), and $k^{7/3}E_M(k)$ (the white circles). Although some scalings other than the $k^{5/3}$ and $k^{7/3}$ have been proposed [8], here we concentrate on studying a possible scaling we have proposed [7]. The kinetic energy spectrum $E_K(k)$ appears to have a scaling by $k^{-5/3}$, as has been pointed out in many works (see Ref. [8] and references therein). On the other hand, $E_M(k)$ may appear two scalings, as has been proposed by the authors, [7] although the scaling regimes are too short and the scalings can not be conclusive. By a comparison of the compensated magnetic energy spectra in Fig.2(a) and (b), the tail of the $E_M(k)$ in the Hall MHD appears less steep than that in the MHD turbulence.

The change of the energy spectra at high wavenumbers of the magnetic field by the Hall effect may be char-

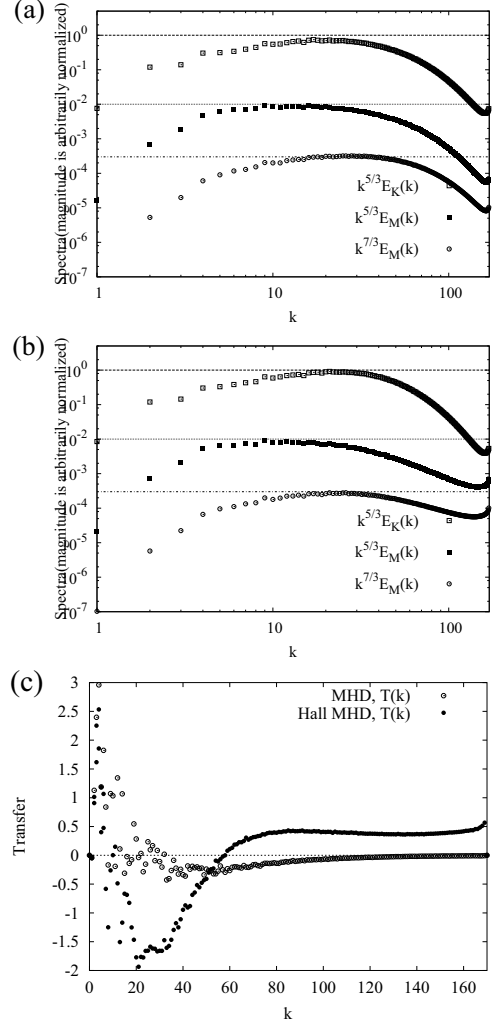


Fig. 2 Kinetic and magnetic energy spectra of (a)MHD and (b)Hall MHD simulations. The spectra are compensated as $k^{5/3}E_K(k)$, $k^{5/3}E_M(k)$ and $k^{7/3}E_M(k)$. Magnitudes of the spectra are normalized by appropriate values so that they can be distinguished from each other clearly. (c)The energy transfer functions of the MHD and the Hall MHD simulations.

acterized by the energy transfer function $T(k)$ [8, 9] which describes the conservative energy transfer among various wavenumber k by the nonlinear terms. In Fig.2(c), the energy transfer function for the total energy $E_K(k) + E_M(k)$ of both the MHD and the Hall MHD simulations are shown. In the MHD case, $T(k)$ is positive at small k and negative at large k , suggesting that the backward energy transfer from larger to lower wavenumbers are dominant at this time of the simulation. On the other hand, in the Hall MHD case $T(k)$ is negative at $10 \leq k \leq 50$ and positive at both $k < 10$ and $k \geq 50$. The transfer $T(k)$ is large and positive especially at the large wavenumber regions, making the resolution of this simulation being marginal. (Recall that the Fourier coefficients at the high wavenumber regime is damped by the viscous and the Ohmic dissipation terms, which are not plotted here.) The difference of $T(k)$

between the two simulations clearly shows that the Hall effects change the energy transfer. In the Hall MHD turbulence, the scales comparable to $1/\epsilon$ becomes the source of the energy which is distributed to the two wavenumber regimes $k < 10$ and $k > 50$. The positive $T(k)$ at $k < 10$ in the Hall MHD turbulence is not reported in our early work [7], probably because the Hall parameter $\epsilon = 0.1$ in the reference is too large to allow the positive $T(k)$ at the largest scales.

3. Local structures

In order to see the influences of the modification of the energy transfer by the Hall effect in Fig.2(c), we observe spatial structures in the real (Cartesian-coordinated) space. Though the authors have seen the structures simply by drawing the isosurfaces of the enstrophy density and current density [7], it is difficult to clarify the Hall effect among many pieces of isosurfaces. In this article, aiming at clarifying the large and scale structures, we introduce the low-pass ($< k_{cut}$) and high-pass ($> k_{cut}$) filters. By the use of filters a field quantity can be separate into the lower-wavenumber and higher-wavenumber components. The cut-off wavenumber is set $k_{cut} = 50$, where $T(k)$ of the Hall MHD turbulence changes its sign.

In Fig.3, isosurfaces of the lower-wavenumber vorticity components $(\omega^{<k_{cut}})^2$ of (a)the MHD and (b)the Hall MHD are drawn. The threshold of isosurface in the figures is twice of the deviation above the mean value of ω^2 . A comparison between Fig.3(a) and (b) reveals that the vorticity field with the wavenumber $k < k_{cut}$ is more tubular in the Hall MHD turbulence than in the MHD turbulence. The change of the structures are not easily found without introducing the filters, since the fine structures of the vorticity are dominant when we plot ω^2 . The change may be related to the $T(k)$ being positive for $k < 10$ and negative for $k > 10$. The dominance of tubular structures in Fig.3(b) suggests that swirling motions are superior to the shearing motions in the large scales due to the Hall effects, like the vortical structures in the Navier-Stokes turbulence [10, 11], although much more detailed analysis is require for further studies.

Fig.4(a) and (b) are isosurfaces of the higher components $(\omega^{>k_{cut}})^2$ of the MHD and the Hall MHD, respectively. The threshold is the same as the value for Fig.3. We find that the the sheet-like structures of the vorticity are torn into pieces in the Hall MHD turbulence.

In Figs.5, isosurfaces of the higher components of the current of (a)the MHD and (b)the Hall MHD simulations are drawn. (The lower components are omitted because we do not observe a significant difference between the MHD and the Hall MHD turbulence.) In comparison to Fig.5(a), the isosurfaces in Fig.5(b) are apparently torn into pieces, forming very fine structures. In the case of the current density field, the Fourier amplitudes of the Hall MHD turbulence are apparently larger than those of the MHD tur-

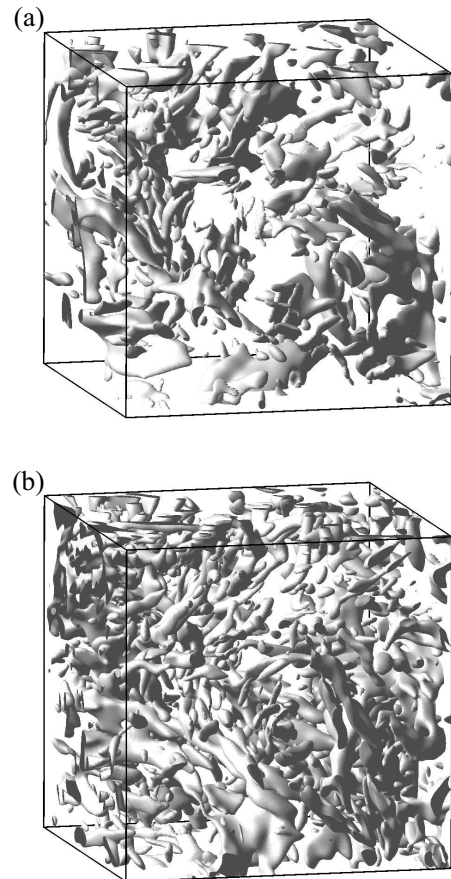


Fig. 3 Isosurfaces of $(\omega^{<k_{cut}})^2$ of (a)the MHD simulation at $t = 1$ and (b)the Hall MHD simulation at $t = 1.04$. The isosurfaces are drawn over a region with 170^3 grid points out of the entire 512^3 region.

bulence, more than one degree of magnitude. (The amplitudes of the vorticity Fourier coefficients of the MHD simulation are slightly larger than those in the Hall MHD turbulence at $k > 80$, although the difference of the amplitudes are very small.) The fine structures in Fig.4(b) may be attributed to the $\mathbf{j} \times \mathbf{B}$ -force in eq.(1), that is, the fine structures in the vorticity (and therefore in the velocity) fields are excited in association with the emergence of the fine structures in the magnetic field. It appears that the Hall term influences the high wavenumber region of the magnetic field and the excited small scales of the magnetic field then influences the small scales of the velocity field.

4. Concluding remarks

We have studied both the scaling properties and the local structures of the Hall MHD turbulence through direct comparisons to the single-fluid MHD turbulence with the same initial condition and the same dissipative parameters. The DNS results appear being consistent with the scaling proposed by Hori and Miura [7]. For the observations of the local structures, the introduction of the low-pass and high-pass filters work satisfactory. The observations of the

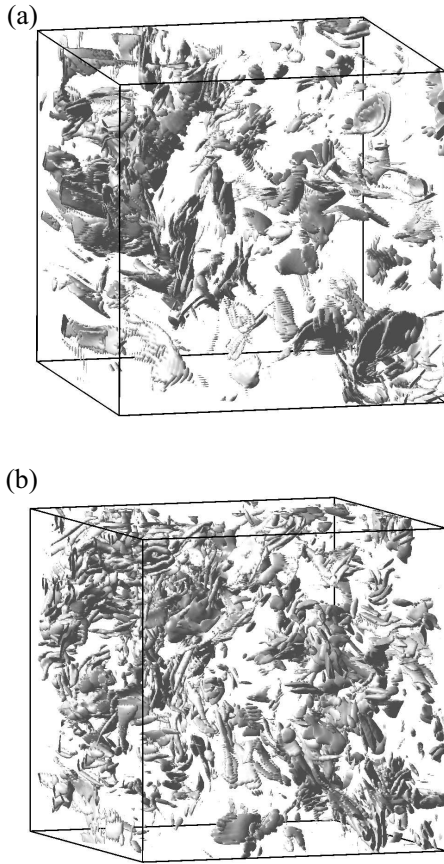


Fig. 4 Isosurfaces of $(\omega^{>k_{cut}})^2$ of (a)the MHD simulation at $t = 1$ and (b)the Hall MHD simulation at $t = 1.04$.

vorticity field suggest that the vortex structures are significantly modified by the Hall effect from sheets to tubes. A tubular vortex is often formed through rolling-up of a vortex sheet due to the Kelvin-Helmholtz (KH) instability. However, it does not directly explain the difference of the vortex structures in between the MHD and the Hall MHD turbulence unless the Hall effects on the KH instability is shown. Concerning an effect which exists in the Hall MHD turbulence but does not in the MHD turbulence, we would like to comment on the Whistler waves. In MHD turbulence, propagations and collisions of the Alfvén waves along the magnetic field lines bring about the modifications of the nonlinear interactions from the Navier-Stokes turbulence and therefore of the spatial structures, too. (See Ref. [8], for example.) In the Hall MHD turbulence, high-wavenumber Whistler waves propagate along the magnetic field lines faster than the Alfvén waves and causes many more collisions. We speculate that the wave collisions may be related to the structure modifications, since many of these structures are observed being tangential to the magnetic field lines (figures are omitted due to the page limitation). It remains as a simple speculation here and will be studied more extensively with a detailed analysis on each of tubular vortices as are carried out in Ref. [10, 11].

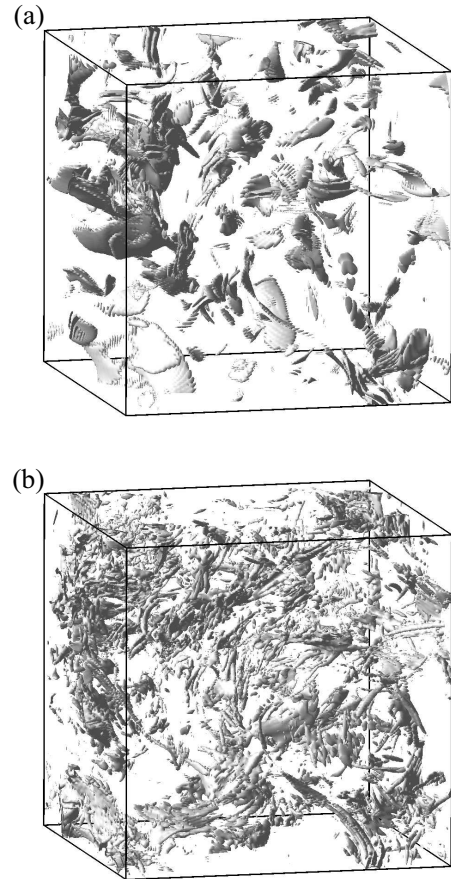


Fig. 5 Isosurfaces of $(j^{>k_{cut}})^2$ of (a)the MHD simulation at $t = 1$ and (b)the Hall MHD simulation at $t = 1.04$.

This research was partially supported by "Application of Fusion Theory to Space Plasmas" under the project of Formation of International Network for Scientific Collaborations at National Institute for Fusion Science (NIFS)/National Institute for Natural Sciences, Japan. The numerical work was performed on the NEC SX-7 "Plasma Simulator" of NIFS.

- [1] K. Itoh, K. Halides, and et. al., Phys. Plasmas **12**, 062303 (2005).
- [2] S. M. Mahajan and Z. Yoshida, Phys. Plasmas **7**, 635 (2000).
- [3] S. Balbus and C. Terquem, Astrophys. J. **552**, 235 (2001).
- [4] J. Shiraishi, S. Ohsaki, and et. al., **12**, 092901 (2005).
- [5] P. D. Mininni, D. O. Gómez, and S. M. Mahajan, Astrophys. J. **619**, 1019 (2005).
- [6] P. Mininni, A. Alexakis, and A. Pouquet, J. Plasma Phys. **73**, 377 (2007).
- [7] D. Hori and H. Miura, to appear in Plasma Fusion Res. (2008).
- [8] D. Biskamp, *Magnetohydrodynamic Turbulence*, Cambridge University Press, 2003.
- [9] W.D. McComb, *The Physics of Fluid Turbulence*, Oxford University Press, 1990.
- [10] H. Miura and S. Kida, J. Phys. Soc. Japan, 1331 **66** (1997)
- [11] H. Miura, J. Turbulence **5** (2004) N10.